DISTURBANCE FEED FORWARD CONTROL OF A HANDHELD PARALLEL ROBOT

Achim Wagner, Matthias Nübel, Essam Badreddin
Automation Laboratory
University of Mannheim, D-68131 Mannheim, Germany
a.wagner@ti.uni-mannheim.de

Peter P. Pott, Markus L. Schwarz
Laboratory for Biomechanics and experimental Orthopaedics, OUZ
Faculty of Medicine Mannheim, University of Heidelberg, Germany

Keywords: Robotic manipulators, Medical systems, Dynamic modelling, Disturbance rejection, Feedforward compensation.

Abstract: A model-based control approach for a surgical parallel robot is presented, which combines a local tool stabilization with a global disturbance feed forward control. The robot is held in the operator's hand during the manipulation of bones. For a precise processing the tool has to be decoupled from disturbances due to unintentional hand movements of the surgeon at the robot base. The base disturbances are transformed for a feed forward control using the inverse dynamics of the robot. Simulations show that disturbances can be reduced by many orders depending on sensor errors and delay.

1 INTRODUCTION

Parallel robots are widely used, where high stiffness, high dynamics or low error propagation over the kinematic chains is required, e.g. flight simulators (Koekebakker et al., 1998), processing machines (Tönshoff et al., 2002), positioning and stabilization platforms (Huynh, 2001), vibration isolation (Chen and McInroy, 2004) and medical manipulators (Pott et al., 2004; Wagner et al., 2004). The probably most famous Hexapod parallel kinematic structure is the Stewart-platform (Stewart, 1966) which has six degrees-of-freedom (DOF). An obvious advantage considering hand-held applications is, that a parallel robot has high potential for a lightweight construction. By fixing the most massive part of the actuators to base (Merlet, 2000), the actively positioned mass can be further decreased. This leads to a reduction of static and dynamic forces (Honegger et al., 1997; Huynh, 2001). The forces of the actuators can be transferred to the tool platform using light struts. Within the hand-held surgical robot project "Intelligent Tool Drive" (ITD), a parallel robot is designed to align a milling tool relatively to a moving bone of the patient (workpiece) and to decouple the tool from unintentional hand movements at the base. The standard procedure to control a parallel manipulator is transforming the desired tool motion into the desired leg motion with the inverse kinematics and controlling the leg motion separately on the axes level (Tönshoff et al., 2002). However, if high dynamics is required this simple kinematics approach does not lead to a high precision tool pose control, especially if the robot's base is freely movable. Therefore, full dynamic models of special parallel robots are introduced to improve the quality of a fast platform control (Riebe and Ulbrich, 2003; Honegger, 1999). The nonlinear inverse dynamic large-signal model for a parallel robot with two movable platforms is introduced in (Wagner et al., 2006). This model is used here to control the pose of the tool, while it is decoupled from base disturbances. Since the robot is movable freely in space adequate co-ordinate systems must be defined. The local control of the tool is performed in the base instantaneously coincident reference frame using the inverse kinematics description of the robot. The same reference frame can be used to achieve a dynamic feed forward compensation. However, for the compensation of the gravity influences and for a absolute position referencing a world coordinate system must be defined. In the following sections the control structure and simulations are presented to show the advantages and drawbacks of the approach.

2 SYSTEM DESCRIPTION

The goal of the ITD robot project is to adjust and to stabilize a drilling or milling tool (mounted at the tool platform) with respect to a moving bone of the patient (workpiece), while the complete machine is held in the surgeon's hand. Therefore it is necessary to isolate the tool from disturbances at the base produced by the operator's unintional hand movements. The amplitude and frequency of the human arm disturbances is available from literature (Takanokura and Sakamoto, 2001). Corresponding to the milling process with different tools a 6 DOF control of the tool is required. Assuming an additional safety margin the selected workspace of the robot ranges from -20 mm to +20 mm in the three Cartesian axes and respectively from -20^o to +20^o in the three rotational axes.

The mechanical device designed is a parallel robot with six base-fixed actuators. The CAD model of the surgical robot ITDII (Intelligent Tool Drive II) is shown in Fig. 1. The robot base has six fixed linear motors, i.e. the electrical part of the motors. Furthermore, there are guide rails, housing, and handles for the hand-held operation, building together the robot base. The sliders of the linear motors are connected to the tool platform via six lightweight struts. At the tool platform and at the sliders the struts are mounted with spherical joints.

Because the base of the robot can be moved freely

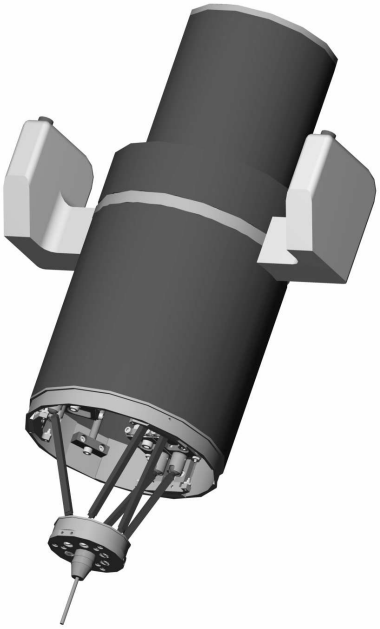

Figure 1: Hand-held surgical robot ITDII - CAD model.

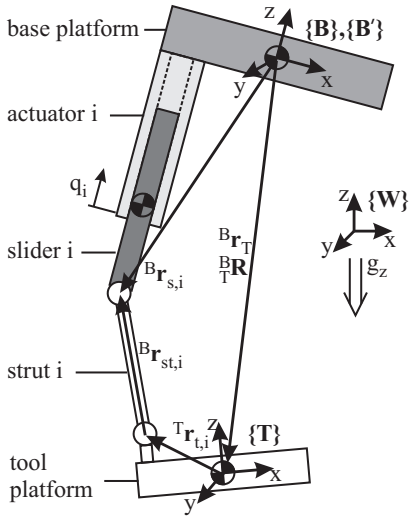

Figure 2: Topology of the parallel robot with fixed actuators.

in space, adequate coordinate systems have to be defined. For the calculation of the kinematic equations four coordinate frames are considered (Fig. 2): (1) the world (earth) frame {W}, (2) the tool frame {T} in the tool's centre of gravity, (3) the movable base frame {B} in the base's center of gravity, and (4) the instantaneously coincident base frame {B'}, which is fixed in {W}. The frame {B'} and the frame {B} are aligned, if the base stands still. Without loss of generality the motion of both platforms is represented in the {B'} frame, which reduces the complexity of the kinematic description. The choice of the coordinates has no influence on the value of the inertial forces. For simplicity the gravity is calculated in the world frame. Afterwards, the resulting force can be transformed into the {B'} frame with little effort.

The pose of the tool is defined by the position vector $^B\mathbf{r}_T$ and the orientation matrix $^B_T\mathbf{R}$ in the {B} frame, which build together the pose vector $^B\mathbf{X}_T = (^B\mathbf{r}_T, {}^B_T\mathbf{R})$. From the matrix $^B_T\mathbf{R}$ the fixed zyx-Euler angles ϕ, θ, and ψ can be derived. The positions of the tool joints $^T r_{t,i}$ in the tool frame and the initial positions of the slider joints $^B r_{s_0,i}$ in the base frame for each actuator i are known from the geometry of the construction. The sliders actual positions $^B r_{s,i}$ move in z-direction of the base according to the guidance, if the tool changes its position. Therefore, the initial positions $^B r_{s,i,x} = {}^B r_{s_0,i,x}$ and $^B r_{s,i,y} = {}^B r_{s_0,i,y}$ in the x-direction respectively the y-direction are not alternated. The struts have the lengths l_i.

3 MODELLING

For the model-based control of the robot, the non-linear inverse dynamic description is required, especially if both platforms can be moved freely in the entire workspace.

3.1 Inverse Kinematics

The inverse kinematics of the robot describes the non-linear relationship between the relative tool-base pose and the slider positions, which states the operating point of the robot in the instantaneously coincident base frame {B'}. Furthermore, the velocities and accelerations of the sliders are given from the relative motion of the tool and the base in {B'}.

3.1.1 Pose

Since the slider positions are constrained by the six struts $i = 1..6$, the joint x and y distances between slider and strut joints are given by

$$ {}^{B}r_{st,i,x} = {}^{B}r_{s,i,x} - {}^{B}r_{t,i,x} \tag{1}$$

and

$$ {}^{B}r_{st,i,y} = {}^{B}r_{s,i,y} - {}^{B}r_{t,i,y}. \tag{2}$$

With the assumption of constant strut lengths l_i the z-component of the joint distance vectors can be calculated as

$$ {}^{B}r_{st,i,z} = \sqrt{l_i^2 - ({}^{B}r_{st,i,x})^2 - ({}^{B}r_{st,i,y})^2} \tag{3}$$

and the slider joint positions yield

$$ {}^{B}r_{s,i,z} = {}^{B}r_{t,i,z} + {}^{B}r_{st,i,z}. \tag{4}$$

The required shift of the actuator positions with respect of the starting positions ${}^{B}r_{s_0,i,z}$ is

$$ q_i = {}^{B}r_{s,i,z} - {}^{B}r_{s_0,i,z}, \tag{5}$$

which is measured by local positioning sensors.

3.1.2 Velocity

The generalized tool and base velocities ${}^{B'}\dot{\mathbf{X}}_T = ({}^{B'}\mathbf{v}_T, {}^{B'}\omega_T)$ and ${}^{B'}\dot{\mathbf{X}}_B = ({}^{B'}\mathbf{v}_B, {}^{B'}\omega_B)$ embrace the translational velocities ${}^{B'}\mathbf{v}_T$ respectively ${}^{B'}\mathbf{v}_B$ and the angular velocities ${}^{B'}\omega_T$ and ${}^{B'}\omega_B$ of both rigid bodies. According to a rigid body motion the tool joint positions and the base-fixed initial slider joint positions can be determined from the generalized velocities. Due to the constant strut lengths, the z-components of the relative slider velocities

$$ {}^{B'}v_{st,i,z} = -\frac{{}^{B}r_{st,i,x}}{{}^{B}r_{st,i,z}}\,{}^{B'}v_{st,i,x} - \frac{{}^{B}r_{st,i,y}}{{}^{B}r_{st,i,z}}\,{}^{B'}v_{st,i,y} \tag{6}$$

result from the constraint movement on a sphere with radius l_i. The relative velocities of the sliders, which can be measured and controlled on the actuator level, is

$$ \dot{q}_i = {}^{B'}v_{st,i,z} + {}^{B'}v_{t,i,z} - {}^{B'}v'_{s,i,z} \tag{7}$$

with the tool joint velocities ${}^{B'}v_{t,i,z}$ and the velocities of the initial joint positions ${}^{B'}v'_{s,i,z}$.

3.1.3 Acceleration

Corresponding to the velocity derivation, the generalized accelerations of the tool and the base are defined by ${}^{B'}\ddot{\mathbf{X}}_T = ({}^{B'}\mathbf{a}_T, {}^{B'}\alpha_T)$ and ${}^{B'}\ddot{\mathbf{X}}_B = ({}^{B'}\mathbf{a}_B, {}^{B'}\alpha_B)$ with the translational accelerations ${}^{B'}\mathbf{a}_T$ and ${}^{B'}\mathbf{a}_B$ and the angular accelerations ${}^{B'}\alpha_T$ and ${}^{B'}\alpha_B$. The accelerations of the joints are assemblies of three terms: (1) inertial acceleration a', 2) centripetal acceleration a'', and (3) Coriolis acceleration a'''. The inertial terms of the slider joints are

$$ {}^{B'}\mathbf{a}'_{s,i} = {}^{B'}\mathbf{a}_B + {}^{B'}\alpha_B \times {}^{B}\mathbf{r}_{s,i}, \tag{8}$$

and the centripetal accelerations are

$$ {}^{B'}\mathbf{a}''_{s,i} = {}^{B'}\omega_B \times {}^{B'}\omega_B \times {}^{B}\mathbf{r}_{s,i}. \tag{9}$$

The Coriolis acceleration terms are non-zero in x-direction

$$ {}^{B'}a'''_{s,i,x} = 2 \cdot {}^{B'}\omega_{B,y} \cdot \dot{q}_i \tag{10}$$

and in y-direction

$$ {}^{B'}a'''_{s,i,y} = -2 \cdot {}^{B'}\omega_{B,x} \cdot \dot{q}_i. \tag{11}$$

The z-component ${}^{B'}a'''_{s,i,z}$ is identical zero.

Summarizing the three terms, the slider joint accelerations in x and y direction result in

$$ {}^{B'}a_{s,i,x} = {}^{B'}a'_{s,i,x} + {}^{B'}a''_{s,i,x} + {}^{B'}a'''_{s,i,x} \tag{12}$$

$$ {}^{B'}a_{s,i,y} = {}^{B'}a'_{s,i,y} + {}^{B'}a''_{s,i,y} + {}^{B'}a'''_{s,i,y}. \tag{13}$$

The slider acceleration in z-direction is not a simple sum, because the slider motion is constrained by the struts according to the sphere equation

$$ \begin{aligned} {}^{B'}a_{st,i,z} = &-\frac{{}^{B}r_{st,i,x}}{{}^{B}r_{st,i,z}}\left({}^{B'}a_{st,i,x} + {}^{B'}a_{nst,i,x}\right) \\ &-\frac{{}^{B}r_{st,i,y}}{{}^{B}r_{st,i,z}}\left({}^{B'}a_{st,i,y} + {}^{B'}a_{nst,i,y}\right) \\ &-\left({}^{B'}a_{nst,i,z}\right) \end{aligned} \tag{14}$$

with the normal acceleration

$$ {}^{B'}\mathbf{a}_{nst,i} = -\left({}^{B}\mathbf{r}_{st,i} \times {}^{B'}\mathbf{v}_{st,i}\right) \times {}^{B'}\mathbf{v}_{st,i} \,/\, \left({}^{B}\mathbf{r}_{st,i}\right)^2 \tag{15}$$

Finally, the slider joint accelerations are

$$ {}^{B'}a_{s,i,z} = {}^{B'}a_{st,i,z} + {}^{B'}a_{t,i,z}. \tag{16}$$

and the acceleration of a slider's center of gravity yields

$$ {}^{B'}a_{cg,i,z} = {}^{B'}a_{s,i,z} + {}^{B'}\omega_B \times {}^{B'}\omega_B \times {}^{B}\mathbf{r}_{scg,i} \qquad (17) $$

with the position offset ${}^{B}\mathbf{r}_{scg,i}$ between the slider joint position and the slider's centre of gravity.

3.2 Inverse Dynamics

The inverse dynamics of the robot describes the actuator forces needed to move the tool's centre of gravity with a desired velocity and acceleration. Additionally, the actuator forces are derived to stabilize the tool, if the base is disturbed. In this section a brief sketch of the ITDII robot's inverse dynamics is given. A more detailed description can be found in (Wagner et al., 2006).

The rigid body dynamics of a parallel robot can be described generally by the equation of motion

$$ {}^{B'}\Lambda_T = \mathbf{M}(\mathbf{q}) \cdot \ddot{\mathbf{q}} + \mathbf{C}(\mathbf{q}, \dot{\mathbf{q}}) \cdot \dot{\mathbf{q}} + \mathbf{G}(\mathbf{q}). \qquad (18) $$

with the generalized force ${}^{B'}\Lambda_T$, which is necessary to move the tool platform in a fixed frame $\{\mathrm{B'}\}$. Within this equation $\mathbf{M}$ is the generalized mass matrix, $\mathbf{C}$ is the centripedal and Coriolis component and $\mathbf{G}$ is the gravity component of the platform. These parameters depend on the operationg point of the robot. The generalized force is converted into actuator forces using the Jacobian matrix of the robot. Additionally, the inertia forces

$$ \mathbf{F}_{s,i} = m_{s,i} \left[{}^{B'}a_{cg,i,z} - \left({}^{B}_{W}\mathbf{R}\,\mathbf{g} \right)_z \right]. \qquad (19) $$

are taken into acount with the slider masses $m_{s,i}$. The gravitiy vector $\mathbf{g} = (0\ 0\ -9{,}81\,m/s^2)^T$ can be transformed from the $\{\mathrm{W}\}$ frame into the $\{\mathrm{B}\}$ frame using the rotation matrix ${}^{B}_{W}\mathbf{R}$. Since the major part of the strut masses is concentrated in the joints and since the link beetween the joints is lightweight, the struts can be separated into two parts, which can be added to the slider and tool components (Honegger, 1999). Correspondingly the strut masses and inertias are not considered in the inverse dynamics explicitly. In a first attempt the friction forces are neglected as well. The latter can easily be extended on the actuator level, if necessary. The non-working reaction forces/torques of the actuators are perpendicular to the actuator motions and, therefore, not considered in the robot dynamics.

For the calculation of all force components the relative velocity and acceleration between the tool and the base as well as the absolute orientation of the robot in the world coordinates must be available. It should be mentioned, that the actuator forces are not simple vector sums of the tool and the base related forces, since the equation of motion is non-linear. However, if the tool is fixed, the ${}^{B'}\Lambda_T$ term vanishes and the remaining forces for the slider mass acceleration yields a quite simple form (19).

4 CONTROL STRUCTURE

The robot control must be suited to adjust the tool against a movable workpiece and to decouple the tool from disturbances at the base. Therefore, a control structure was designed, which combines a servo control on the local axis level with a disturbance feed-forward control in the global Cartesian space (Fig. 3).

For the controller design the adequate choice of co-ordinate systems is essential, since the complete robot can be moved freely in space and the component inertia forces are related to a earth fixed (respectively inertia) reference system. The local stabilization is based on the robot kinematics, which describes the relative pose between tool and base in relation to the actuator positions. Here, the actuator position are not dependent on the tool and base reference. In contrast, the feed-forward control uses the inverse dynamics block, which is definded in $\{\mathrm{B'}\}$. The sensor signals for the base pose, velocity and acceleration are retrieved in the world frame. Furthermore, the desired tool motion is given in the world frame as well. Therefore, the tool and base motion signal are converted to $\{\mathrm{B'}\}$ co-ordinates before they are applied to the inverse kinematics. This geometric transformation can be done with little effort.

The local control is based on the slider position and velocity sensor signals $\mathbf{q}$ and $\dot{\mathbf{q}}$. The actuator signals are compared to the desired actuator signals $\mathbf{q_d}$ and $\dot{\mathbf{q}}_\mathbf{d}$. Using the generalized tool mass matrix $\mathbf{M}$ a PD-controller generates the force signals $\mathbf{F_{fb}}$ needed to stabilize the tool. The reference signals $\mathbf{q_d}$ and $\dot{\mathbf{q}}_\mathbf{d}$ result from the desired tool signals ${}^{W}\mathbf{X}_{Td}$, and ${}^{W}\dot{\mathbf{X}}_{Td}$ and from the actual base coordinates ${}^{W}\mathbf{X}_{B}$, and ${}^{W}\dot{\mathbf{X}}_{B}$ both in Cartesian world coordinates, using the inverse kinematics of the parallel robot.

The feed-forward control block consists of two inputs, the tool reference signals ${}^{W}\mathbf{X}_{Td}$, ${}^{W}\dot{\mathbf{X}}_{Td}$, and ${}^{W}\ddot{\mathbf{X}}_{Td}$ and the actual base signals ${}^{W}\mathbf{X}_{B}$, ${}^{W}\dot{\mathbf{X}}_{B}$, and ${}^{W}\ddot{\mathbf{X}}_{B}$. Using the inverse dynamic model the feed-forward forces $\mathbf{F_{ff}}$ are calculated which are required to move the tool as desired, while the disturbances from the base are canceled. If the inverse dynamic model and the sensor/actuator signals are assumed to be perfect, the local control error will be zero. However, the inverse model is not really complete due to the neglected strut masses, actuator friction and un-

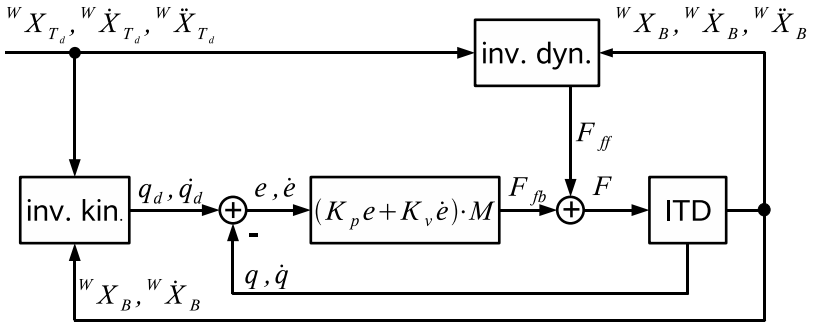

Figure 3: Control structure; local servo loop and global disturbance feed forward control.

measured disturbances. These model uncertainties are compensated by the local pose control. The presented structure is not a classical cascaded structure, because the base coordinates are not influenced immediately by the control action. The base motion results from the disturbance forces of the human operator. That means that no feed-back from the actuators to the base motion is assumed due to the large base mass and that the sensing of the base motion serves for the referencing of coordinates only.

In the realized system it is necessary to measure the pose, the velocity and the acceleration of the base. The tool coordinates are calculated from the desired tool trajectory. To take care of force feed-back during the processing of the workpiece, additional sensors measuring the tool motion or forces could be implemented in a feed-back control. This may make sense in special cases. However, backlash effects in the joints could lead to a destabilization of the controlled system. Therefore, and for the sake of simplicity we are content with the local stabilization.

As shown in literature (Riebe and Ulbrich, 2003), a friction compensation is essential in the real application, which can be added on the local axis level. To separate the kinetic effects from the friction effects, such a compensation is neglected in this paper. The control structure has been implemented in the simulation environment Matlab/Simulink using a fixed sampling time of 1 ms. As a consequence the minimum delay in the control loop is 1 ms as well. The forward dynamics of the robot ITD used in the closed loop simulations has been modelled with the SimMechanics toolbox.

5 SIMULATION

The simulations presented in this section mainly support the description of the disturbance decoupling ability of the system. Additionally, the overall trajectory tracking quality is described at the end using a standard circle test (ballbar-test).

5.1 Tool Stabilization

The first simulations describe the system disturbance response in the frequency domain. In the first simulations the control parameters are configured for a critically damped PD control loop with a system frequency $\Omega = 60Hz$. Figure 4(a) shows the tool motion after application of a 12 Hz, 1 mm sinusoidal signal at the base. The straight line represents the stimulus in the x-direction, which can be referenced to the left hand scale. The amplitude of the tool position response using a PD control (dotted line) and using a PD control with additional feed forward disturbance

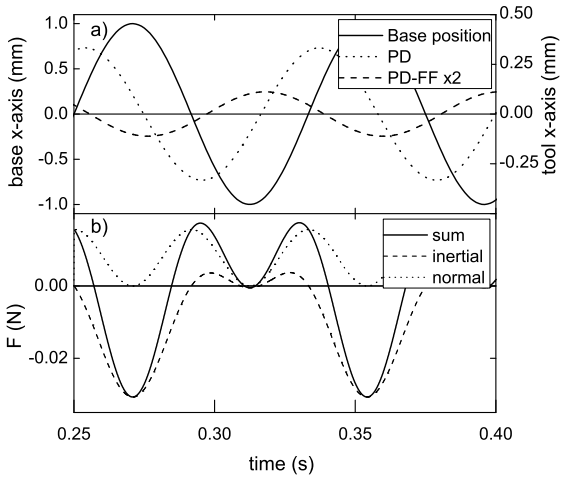

Figure 4: Response on a 12 Hz, 1 mm sinusoidal translational base disturbance in x-axis; (a) base position stimulus (straight line, left-hand scale), tool position response (PD control, dotted line, right-hand scale), tool position response multiplied by a factor of two (PD control with disturbance feed-forward, dotted line, right-hand scale); (b) Force needed for feed-forward compensation.

compensation (dashed line) can be extracted from the right hand scale. For a better readability the later is multiplied by a factor of two.

As a result the PD controlled tool is damped against the base disturbance with a transfer factor of 0.3 (-10dB) due to its limited bandwidth. Adding the feed-forward control the transfer factor decreases to 0.06 (-24dB).

The actuator force needed to cancel the disturbances is plotted in Fig. 4(b) for the first actuator. The resulting force F (straight line) is the total of all force components. The inertial component (dashed line) results from the tool and the slider acceleration (8) and the normal component (dotted line) is a consequence of the strut rotation velocity (6). No Coriolis or centripedal forces are generated for a translational tool movement. While the tool-pose reaction seams to be more or less a sinusoidal function, higher harmonic distortions are noticeable in the inertial component.

Now, the sinusoidal stimulus is shifted to 1 Hz and 20 mm amplitude (Fig. 5) compared to Fig. 4. Here, the feed-forward related position response is multiplied by a factor of 50. As a result of the lower frequency the PD-loop has an increased damping effect with a transfer factor of $6 \cdot 10^{-3}$ (-45dB) respectively $6.5 \cdot 10^{-5}$ (-84dB) with feed forward control (Fig. 5). The pose response signal in the large signal case is not a sinusoidal signal anymore due to the non-linear coupling between tool and base.

A sinusoidal stimulation of the base orientation

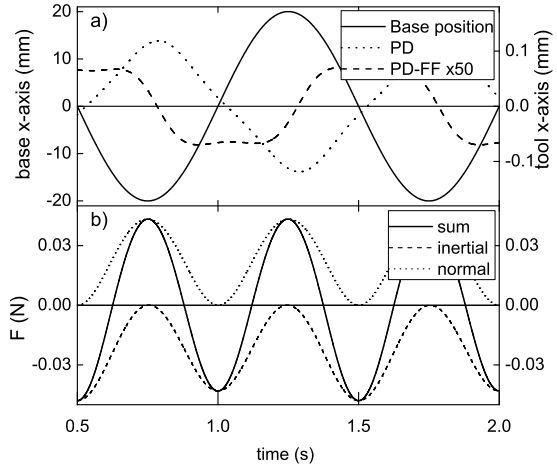

Figure 5: Response on a 1 Hz, 20 mm sinusoidal translational base disturbance in x-axis; (a) base position stimulus (straight line, left-hand scale), tool position response (PD control, dotted line, right-hand scale), tool position response multiplied by a factor of 50 (PD control with disturbance feed-forward, dotted line, right-hand scale); (b) Force needed for feed-forward compensation.

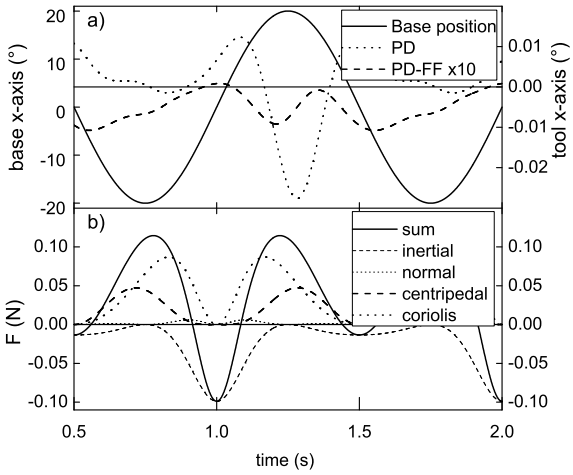

Figure 6: Response on a 1 Hz, 20^o sinusoidal rotational base disturbance around the x-axis; (a) base orientation stimulus (straight line, left-hand scale), tool orientation response (PD control, dotted line, right-hand scale), tool orientation response multiplied by a factor 10 (PD control with disturbance feed-forward, dotted line, right-hand scale); (b) Force needed for feed-forward compensation.

around the x-axis and its response is shown in Fig. 6(a). The forces needed to stabilize the tool are plotted in Fig. 6(b). Here, the Coriolis (large dotted line) and centripedal (large dashed line) forces are in the range of the inertia forces. Unlike an intuitive estimation the Coriolis and centripedal components cannot be neglected in this special robot application.

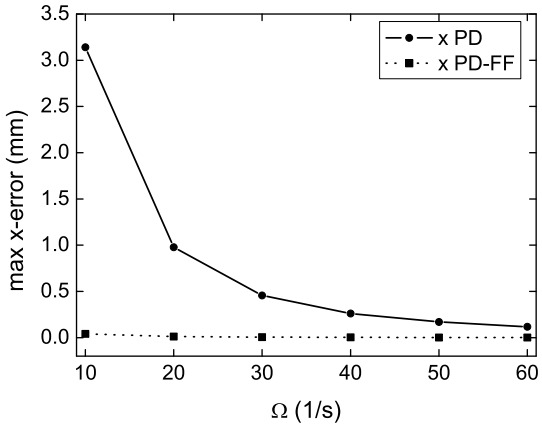

Figure 7: x- axis response on a 1 Hz, 20 mm sinusoidal translational base disturbance in dependence on the servo loop frequency.

The decoupling behaviour from the base motion strongly depends on the choice of the parameter Ω and the delay in the feed-back loop, which is at least one sampling period. This is shown in Fig.7 and Fig.8

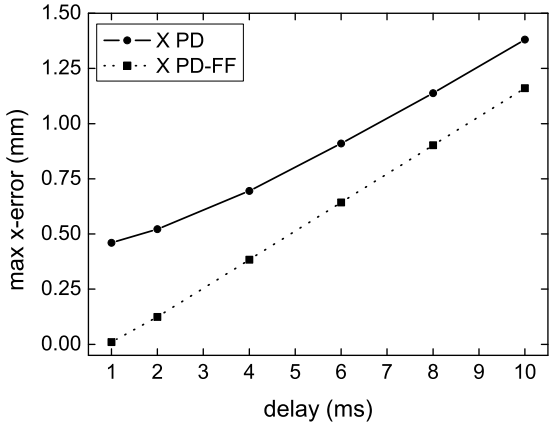

Figure 8: x- axis response on a 1 Hz, 20 mm sinusoidal translational base disturbance in dependence on the sensor delay.

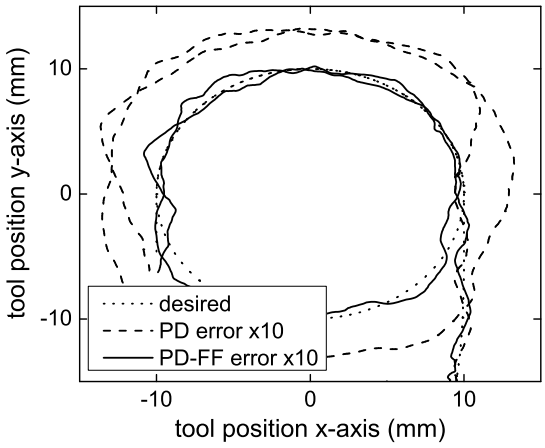

Figure 9: Standard circle test with white Gaussian sensor noise; $\sigma_{accel} = 0.17 mm/s^2$ translational standard deviation, $\sigma_{rot} = 0.17 rad/s$ rotational standard deviation, $v = 0.1 m/s$ feed speed.

for a base disturbance of 1 Hz and 1 mm.

The pose error amplitude and phase decrease with increasing control loop frequency. With disturbance feed forward control the error is generally smaller, however the quality strongly depends on the sensor delay. To estimate the limit time lack that can be allowed the pose error is plotted against the sensing delay. For instance, the delay should not exceed 3 ms, if a pose accuracy of 0.3 mm is required. (Certainly, additional error sources must be considered).

5.2 Tracking Control

To assess the possibilities of the disturbance feed forward control the standard circle (ballbar) test was simulated assuming an additional white Gaussian sensor noise with a translational standard deviation of $\sigma_{accel} = 0.17 mm/s^2$ and a rotational standard deviation of $\sigma_{rot} = 0.17 rad/s$ for all axes. Figure 9 shows the reference trajectory, which has to be followed with a velocity of 0.1 m/s, and the actual trajectories using a PD control and using a PD control with disturbance feed forward. The deviation from the reference trajectory is exaggerated by a factor of five. The mean pose error are 0.35 mm and 0.10 mm with respectively without feed forward control. The standard deviations are 0.051 mm and 0.052 mm. Also for the reference action the feed forward control diminishes the pose error remarkably. Because the signal noise from the base sensors is injected into the inverse kinematics block as well as into the inverse dynamics block, it influences the PD control loop once and the PD control with feed forward control twice. However, the persistent pose noise is not much larger with a feed forward control compared to the pure PD control approach.

6 DISCUSSION

The simulations show, that if a complete model of the parallel robot and adequate sensor signals are available, a feed forward control can lead to a decoupling from base disturbances with high damping factors. For the quality of the decoupling the sensor noise and the sensor delay are essential. The simulated damping value of $6.5 \cdot 10^{-5}$ in the 1 Hz case (Fig. 5) must be interpreted with care, because the quality of the decoupling is influenced by numerical errors in this range. Furthermore, model uncertainties and sensor errors do not allow such a high precision in real-world applications. Within the control approach the base pose, velocity and acceleration must be measured or observed accurately in the inertia system. This is a serious problem, because not only sensor latency and noise must be considered but also misalignment, bias, drift, etc..

For the simulations an ideal model is assumed without geometric or parametric errors and without considering the friction in the actuators and joints. An enhancement of the dynamic model can be done with acceptable effort, e.g. the modelling of friction on the actuator level. However, the quantity of friction and its influence on the dynamics depends on the special mechanical implementation and many parameters. Therefore a possible model extension must be considered if the robot is realized. In contrast to the intuitive impression that for the size, mass and dynamics of a hand-held robot the Coriolis and centripedal forces do not play any role, the simulations show that these force components make a remarkable

contribution to the total force in the actuators. Thus, a simplification of the model by neglecting the velocity related force components is not suitable. Finally, the simulations show in which range of precision a feed forward control does improve the decoupling behaviour and in which range the feed forward control can be neglected.

7 CONCLUSION

A model-based approach is presented to control the tool pose of a handheld robot and to decouple the tool from base disturbances. An adequate definition of coordinate frames for the dynamics modelling and the controller design reduces the effort for the implementation. The feasibility of a feed-back control on the local axis level in combination with a disturbance feed forward control on the robot level in world coordinates is shown. The local control is able to stabilize the robot and to avoid huge errors due to model uncertainties and disturbances. The feed forward control ensures the free movement of the robot in space, while measured disturbances can be compensated for. Furthermore, the usage of a non-linear inverse dynamics model enables the precise disturbance feed-forward control under different operational conditions. For the feed-forward control sensor error and delay are crucial.

REFERENCES

Chen, Y. and McInroy, J. E. (2004). Decoupled control of flexure-jointed hexapods using estimated joint-space mass-inertia matrix. *IEEE Transactions on Control Systems Technology*, 12.

Honegger, M. (1999). *Konzept einer Steuerung mit adaptiver nichtlinearer Regelung für einen Parallelmanipulator*. Dissertation, ETH Zurich, Switzerland, http://www.e-collection.ethbib.ethz.ch.

Honegger, M., Codourey, A., and Burdet, E. (1997). Adaptive control of the hexaglide, a 6 dof parallel manipulator. *IEEE International Conference on Robotics and Automation, Albuquerque, USA*.

Huynh, P. (2001). Kinematic performance comparison of linar type parallel mechanisms, application to the design and control of a hexaslide. *5th International conference on mechatronics technology (ICMT2001), Singapore*.

Koekebakker, S., Teerhuis, P., and v.d. Weiden, A. (1998). Multiple level control of a hydraulically driven flight simulator motion system. *CESA Conference, Hammammet*.

Merlet, J. (2000). *Parallel robots*. Kluwer Academic Publisher, Dordrecht, Netherlands.

Pott, P., Wagner, A., Köpfle, A., Badreddin, E., Männer, R., Weiser, P., Scharf, H.-P., and Schwarz, M. (2004). A handheld surgical manipulator: Itd - design and first results. *CARS 2004 Computer Assisted Radiology and Surgery, Chicago, USA*.

Riebe, S. and Ulbrich, H. (2003). Modelling and online computation of the dynamics of a parallel kinematic with six degrees-of-freedom. *Archive of Applied Mechanics*, 72:817–829.

Stewart, D. (1965-1966). A platform with six degrees of freedom. *Proceedings of the Institute of Mechanical Engineering*, 180:371–386.

Takanokura, M. and Sakamoto, K. (2001). Physiological tremor of the upper limb segments. *Eur. J. Appl. Physiol.*, 85:214–225.

Tönshoff, H., Grendel, H., and Grotjahn, M. (2002). Modelling and control of a linear direct driven hexapod. *Proceedings of the 3rd Chemnitz Parallel Kinematics Seminar PKS 2002, 2002 Parallel Kinematic Machines Int.Conf.*

Wagner, A., Pott, P., Schwarz, M., Scharf, H.-P., Weiser, P., Köpfle, A., Männer, R., and Badreddin, E. (2004). Control of a handheld robot for orthopedic surgery. *3rd IFAC Symposium on Mechatronic Systems, September 6-8, Sydney, Australia*, page 499.

Wagner, A., Pott, P., Schwarz, M., Scharf, H.-P., Weiser, P., Köpfle, A., Männer, R., and Badreddin, E. (2006). Efficient inverse dynamics of a parallel robot with two movable platforms. *4rd IFAC Symposium on Mechatronic Systems, Heidelberg, Germany*.